Chapter 10

COMPARATIVE CRYSTAL CHEMISTRY OF ORTHOSILICATE MINERALS

Joseph R. Smyth, Steven D. Jacobsen
Department of Geological Sciences, 2200 Colorado Avenue, University of Colorado, Boulder, CO 80309-0399

Robert M. Hazen
Geophysical Laboratory, 5251 Broad Branch Road NW, Washington, DC 20015-1305

INTRODUCTION

The Earth's average mantle composition is presumed to lie between an Si:O atom ratio of 1:3 and 1:4 (e.g., Ita and Stixrude 1992). The orthosilicate group, which comprises minerals that contain isolated SiO_4 tetrahedra, has thus been the subject of considerable structural investigation at elevated temperature or pressure. The group includes olivines, silicate spinels, garnets, the aluminosilicates, zircon and a few minor mineral groups such as humites and datolites (Deer et al. 1997). In addition, the silicate spinelloids are typically included here, but are not strictly orthosilicates as they contain Si_2O_7 dimers. Titanite ($CaTiSiO_5$), though technically an orthosilicate, has a framework structure and is considered in Chapter 12 (Ross *this volume*), which also examines aspects of the garnet framework structure not reviewed here. Interestingly, no natural members of the group contain major amounts of monovalent (alkali) cations, although $LiScSiO_4$ has been synthesized in the olivine structure.

The most geologically significant members of the group are those minerals of formula X_2SiO_4, where X is a divalent cation, typically Mg, Fe, Mn, Ca, and (more rarely) Co and Ni. These groups include the olivines, the silicate spinels and wadsleyite-type spinelloids, plus some minor phases such as phenakite (Be_2SiO_4), willemite (Zn_2SiO_4), and cadmium and chromous orthosilicates. The structures of most of the major members of the group have been studied at elevated temperatures or at elevated pressures, but there have not yet been many studies of structures at simultaneously elevated temperature and pressure.

Other members of the orthosilicate group that are of major geological and geophysical significance are the Al_2SiO_5 aluminosilicate polymorphs (sillimanite, andalusite and kyanite), zircon ($ZrSiO_4$), and the garnets, which are abundant in high-pressure metamorphic rocks. The structures of these phases have been studied at high temperature and/or pressure. However, the structures of several orthosilicates, including the humites (chondrodite, humite, clinohumite and norbergite), staurolite, and datolite, have not yet been investigated at temperature or pressure.

In addition to their geological significance, orthosilicate comparative crystal chemistry is of interest because these structures tend to be relatively dense, with extensive edge sharing among cation coordination octahedra and tetrahedra. As a result, the response of orthosilicate structures to temperature and pressure is often a direct reflection cation polyhedral variations. In particular, orthosilicates consistently demonstrate the relative rigidity of silicate tetrahedra relative to divalent and trivalent cation polyhedra.

A review of orthosilicate comparative crystal chemistry is timely, because the number of published structures at nonambient conditions has increased more than four-fold since the review of Hazen and Finger (1982), when only 16 such articles had appeared. Our main objectives here are to review the mineral structures that have been studied at elevated temperatures and/or pressures, to compile the thermal expansion and compression data for the various structural elements in a consistent fashion, and to suggest opportunities for future work. We have chosen to assume linear expansion coefficients for the thermal expansion of various structural elements, because it facilitates comparison across disparate structures and methodologies. In addition, most reported high-temperature structural data are not sufficiently precise to permit the meaningful derivation and comparison of second-order parameters. For compression data, we have computed linear axial compressibilities to facilitate comparison of the various axes, but have retained the second- or higher-order bulk modulus parameters, K' etc., where they have been refined, or else assumed the standard value of 4 for K'.

OLIVINE GROUP

Olivines are a group of orthosilicate minerals of the general formula X_2SiO_4, where X is a divalent metal cation (Mg, Fe, Mn, Ni, Ca, and Co). Olivine crystal chemistry has been reviewed by Brown (1982). Ferromagnesian olivine is generally thought to be the most abundant phase in the Earth's upper mantle, so the physical properties of this material are a central concern to geophysics. The principal mineral end-members are forsterite ("Fo," Mg_2SiO_4), fayalite ("Fa," Fe_2SiO_4), tephroite ("Te," Mn_2SiO_4), liebenbergite (Ni_2SiO_4), monticellite ($CaMgSiO_4$), kirschsteinite ($CaFeSiO_4$), and glaucochroite ($CaMnSiO_4$). In addition Ca_2SiO_4, Co_2SiO_4, and $LiScSiO_4$ have been synthesized in the olivine structure. Other non-silicate minerals with the olivine structure, including chrysoberyl ($BeAl_2O_4$), lithiophyllite ($LiMnPO_4$), tryphyllite ($LiFePO_4$), and natrophyllite ($NaMnPO_4$), provide additional insights to the behavior of this structure type.

The orthorhombic olivine structure (space group *Pbnm*; Z = 4), illustrated in Figure 1, is based on a slightly expanded and distorted hexagonal close-packed array of oxygens. The quasi-hexagonal layers of oxygen atoms in the *b*-*c* plane are stacked in the *a*-direction. Of the two octahedral sites, M1 is located on an inversion at the origin, and M2 is on the mirror. Si is also on the mirror, as are two of the three oxygen atoms, O1 and O2, while the O3 oxygen atom is in a general position. Each of the oxygens in the structure is bonded to three octahedral cations and one tetrahedral cation, so silicate olivines contain no bridging oxygens and no non-silicate oxygens.

High-Temperature Behavior of Olivines

For silicate olivines, the behavior at elevated temperatures and pressures is and as yet unexplained silicate tetrahedra and the more compliant divalent metal octahedra. At temperature, the forsterite structure has been studied by Smyth and Hazen (1973), Hazen (1976) and Takéuchi et al. (1984). Other end-member olivine structures that have been studied at temperature include fayalite (Smyth 1975), and liebenbergite, monticellite and glaucochroite (Lager and Meagher 1978). High-temperature structural studies of intermediate Fe-Mg olivines include $Fo_{69}Fa_{31}$ (Brown and Prewitt 1973), $Fo_{37}Fa_{55}Te_8$ (Smyth and Hazen 1973; Hazen 1976), $Fo_{13}Fa_{87}$ and $Fo_{70}Fa_{30}$ (Motoyama and Matsumoto 1989), and $Fo_{88}Fa_{12}$ (Artioli et al. 1995). Additional high-temperature structural studies include chrysoberyl (Hazen and Finger 1987), synthetic Ni-Mg olivines (Hirschmann 1992), and $MgMnSiO_4$ and $FeMnSiO_4$ by both neutron and X-ray diffraction methods (Redfern et al. 1997). In addition to structural studies at temperature, numerous measurements of olivine thermal expansion by high-precision X-ray powder diffraction methods have been reported (e.g., Suzuki 1975; see tabulation by Fei 1995).

Linearized thermal expansion parameters are summarized for end-member olivines in Table 1 and for intermediate Fe-Mg olivines in Table 2. Of the various end-members, forsterite appears to be the most expansible, whereas the calcic end-members monticellite and glaucochroite are the least. Linear volume thermal expansion coefficients at one atmosphere range from a low of about 3.0×10^{-5} K^{-1} for monticellite and glaucochroite (Lager and Meagher 1978) to about 4.4×10^{-5} K^{-1} for forsterite (Takéuchi et al. 1984). Thus, for the silicate olivine structure there appears to be an unusual anti-correlation of volumetric thermal expansion with unit cell volume.

For structural studies at temperature, linear volumetric and axial thermal expansion coefficients are presented in Tables 1 and 2 for several representative olivine structures along with polyhedral expansions. In general, the *a*-direction (normal to close-packed layers) is the least expansible, whereas expansion within the close-packed plane is greater. Looking at the effect of increasing temperature on the various coordination polyhedra, we see that the silicate tetrahedron shows only minimal or slightly negative expansion with temperature, whereas the divalent metal octahedra and the non-polyhedral volume take up most of the expansion. The larger M2 polyhedron is more expansible than M1 in all silicate olivines.

The structure of chrysoberyl, an olivine isomorph in which Al occupies the octahedral sites and Be the tetrahedral site, was studied to 690°C by Hazen and Finger (1987). They observed significant expansion of both octahedra and tetrahedra, with similar average linear expansion coefficients of 0.8 and 0.9 (both x 10^{15} K^{-1}) for Al and Be polyhedra, respectively. Interestingly, no natural members of the group contain major amounts of monovalent (alkali) cations, although $LiScSiO_4$ has been synthesized in the olivine structure. for Al and Be polyhedra, respectively. This uniformity leads to nearly isotropic expansion of the unit cell. The *a*, *b*, and *c* axial expansivities are 0.74, 0.85, and 0.83 (all x 10^{15} K^{-1}), respectively.

Ordering of Mg and Fe in ferromagnesian olivines has long been a subject of study, and a complete review of the literature is beyond the scope of this chapter. Useful summaries of recent work are presented by Artioli et al. (1995) and Redfern et al. (1997). Exchange between Mg and Fe occurs rapidly in these structures at temperatures above about 600ºC, so that exchange equilibria can be achieved in times of less than 0.1 s (Akamatsu and Kumazawa 1993). Note that the rapid equilibration of olivine ordered state above 600ºC may complicate *in situ*

equation-of-state and structural studies, for which the changing state of order must be documented carefully at each temperature and pressure.

X-ray investigations of the olivine structure at temperatures up to about 800ºC indicate a slight preference of Fe for the smaller M1 site, however Artioli et al. (1995) report a small but significant preference of Fe for M2 at temperatures above 1000ºC. In contrast to Mg-Fe olivines, ordering of other divalent cations is much more pronounced with Ni showing a strong preference for M1 (Hirschmann 1992), whereas Mn and Ca show strong preference for M2 (e.g., Smyth and Tafto 1982). Redfern et al. (1997) studied Fe-Mn and Mg-Mn olivines at elevated temperature with carefully controlled oxygen fugacity, and concluded that Mg-Fe distributions in natural Mg-Fe olivine can be used for cooling rate indicators for rapidly cooled samples.

High-Pressure Behavior of Olivines

High-pressure structure refinements from single crystals in the diamond anvil cell have been done for several olivine compositions. Forsterite was studied to 5 GPa by Hazen (1976), to 4.0 GPa by Hazen and Finger (1980) with improved data collection and processing procedures, and to 14.9 GPa by Kudoh and Takeuchi (1985). Fayalite was studied to 4.2 GPa by Hazen (1977) and to 14.0 GPa by Kudoh and Takeda (1986). Other high-pressure studies of olivine isomorphs include monticellite to 6.2 GPa (Sharp et al. 1987), chrysoberyl to 6.3 GPa (Hazen 1987), and synthetic $LiScSiO_4$ olivine to 5.6 GPa (Hazen et al. 1996). Although the studies by Kudoh and Takeuchi (1985) and Kudoh and Takeda (1986) went to very high pressures, the crystals appear to have suffered severe anisotropic strain at pressures above 10 GPa.

The compression of the unit cell is strongly anisotropic for all silicate olivine structures (except $LiScSiO_4$-- see below), with the *b*-axis being by far the most compressible in all natural compositions. This compression behavior is consistent with ultrasonic measurements of ferromagnesian olivines, which indicate that *b* is the slowest direction whereas *a* and *c* are nearly equal and fast (Bass 1995). A cursory examination of the structure, illustrated in Figure 1, reveals the cause of this anisotropy. The M2 polyhedra form continuous layers in the *a*-*c* plane so that compression parallel to *b* depends only on compression of the most compressible structural unit, M2, whereas compression in other directions requires compression of both M1 and M2. Further, the M2 polyhedron shares an edge with the silicate tetrahedron, but this shared edge is parallel to *c* so it does not affect compression in the *b*-direction.

A common feature of silicate olivine structural variations with pressure is that the silicate tetrahedra retain their rigidity and generally show very little compression over the ranges studied (Table 2). By contrast, M1 and M2 octahedra display significant compression in all of these phases, and their behavior controls olivine compressional anisotropy.

The close relationship between olivine structure and compression behavior is elucidated by a comparison of the behavior of three olivine isomorphs with different cation valence distributions among M1, M2 and T: $(Mg)^{2+}(Mg^{2+})(Si^{4+})O_4$ [2-2-4] versus $(Al^{3+})(Al^{3+})(Be^{2+})O_4$ [3-3-2] versus $(Li^{1+})(Sc^{3+})(Si^{4+})O_4$ [1-3-4], as described by Hazen et al. (1996). The 2-2-4 olivines display the greatest compressional anisotropy, with *a*:*b*:*c* axial compressibilities approaching 1:3:1 in some compositions, as outlined above. The 3-3-2 chrysoberyl, in which M1, M2, and T polyhedra display more nearly equal compressibilities, is more isotropic, with a 1.0:1.3:1.2 axial compression ratio (Hazen 1987). By contrast, compression of 1-3-4 $LiScSiO_4$ is nearly isotropic (1.00:1.04:0.97), by virtue of the greater compression of Li-occupied M1 and lesser compressibility of Sc-occupied M2, relative to 2-2-4 silicate olivines.

The general effect of increasing pressure on the silicate olivine structure is observed to be similar to that of decreasing the temperature, so that "mantle olivine at 100 km depth is predicted to have a crystal structure similar to that of forsterite at 1 atmosphere and 600ºC" (Hazen, 1977). This inverse relationship between structural changes with increasing pressure versus increasing temperature is particularly well displayed by chrysoberyl, as discussed in Chapter 5 on general crystal chemistry (Hazen and Prewitt, *this volume*).

SILICATE SPINELLOID GROUP

Spinelloids comprise a series of oxide structures that occur in both natural and synthetic Mg-Fe-Ni aluminosilicate systems. They typically contain trivalent cations and may also be potential hosts for hydrogen under pressure-temperature conditions of the Transition Zone (410-670 km depth). The structures of spinelloids I (Ma et al. 1975), II (Ma and Tillmanns 1975), III (Ma and Sahl 1975), IV and V (Horioka et al. 1981a,b) have many features in common. Spinelloid III is isomorphous with wadsleyite, and spinelloid IV is similar, but not identical, to the wadsleyite II structure described by Smyth and Kawamoto (1997). Like spinels, they are based on cubic-close-

packed arrays of oxygen, and they have an ideal formula of M_2TO_4, where M is an octahedral cation, which may have charge +2 or +3, and T is the tetrahedral cation, which may have charge +3 or +4. Unlike spinels and olivines however, all spinelloids have bridging oxygens within Si_2O_7 dimers, and an equal number of non-silicate oxygens. The non-silicate oxygens are potential sites for protonation (Smyth 1987), and spinelloid III (wadsleyite) has been shown to contain up to 3.3 % H_2O by weight (Inoue et al. 1997).

The mineral wadsleyite is $(Mg,Fe)_2SiO_4$ in the spinelloid III structure. Because it is generally thought to be a major phase in the upper portion of the Transition Zone, wadsleyite is by far the best studied of the spinelloid structures. As noted above, the orthorhombic structure (space group *Imma*), illustrated in Figure 2, is not strictly an orthosilicate, but rather a sorosilicate with Si_2O_7 dimers and a non-silicate oxygen (O1). The bridging oxygen (O2) is overbonded and the relatively long cation bonds to O2 are the longest, weakest, and most compressible in the structure. The structure features three distinct octahedral sites, M1, M2, and M3, with M1 being smallest and M2 and M3 slightly larger. In marked contrast to olivine, ordering of Mg and Fe is significant among the sites with Fe preferring M1 and M3 over M2.

In the $(Mg,Fe)_2SiO_4$ binary system, the wadsleyite structure occurs from compositions of pure Fo_{100} to about Fa_{25}, although metastable compositions up to Fa_{40} have been reported (Finger et al. 1993). Hydrous varieties have been reported with a significant deviation from orthorhombic symmetry, with monoclinic space group *I*2/*a* and a unit-cell β angle of 90.4º (Smyth et al. 1997; Kudoh and Inoue 1999). The hydrous varieties have significantly shorter *a* and significantly longer *b* axes and slightly larger cell volumes.

Although there have been no structural studies at elevated temperatures to date, Suzuki et al. (1980) measured the thermal expansion up to 800ºC and showed that *a* is nearly twice as expansible as *b* or *c* (Table 3). Hazen et al. (2000a,b) report atom position data to pressures greater that 10 GPa at room temperature for anhydrous Fo_{100} and Fo_{75} wadsleyites as well as for a synthetic isomorph of formula $Fe^{2+}_{1.67}Fe^{3+}_{0.33}(Fe^{3+}_{0.33}Si_{0.67})O_4$. Their results are summarized in Table 4. Although all three samples have bulk moduli that are nearly identical at 173 GPa, the compressibilities of the various cation polyhedra show significant variations. As in silicate olivines, the silicate tetrahedra are relatively incompressible, whereas divalent cation octahedra display bulk moduli consistent with those in other orthosilicates. In agreement with the earlier unit-cell compression study of Hazen et al. (1990), both of the samples with only Si in the tetrahedral sites show nearly equal compression in the *a* and *b* directions, while *c*–axis compression is about 50% greater. The sample with ferric iron in both tetrahedral and octahedral sites, with preferential ordering of Fe^{3+} in M1 and M3, showed nearly equal compression in all three directions.

At the atomic level all three wadsleyites show relatively incompressible tetrahedral sites. At high pressure the bulk moduli of all three octahedral sites are roughly comparable in the pure Mg end member, but for the Fa_{25} composition, the M2 site is more compressible than either M1 or M3, consistent with its higher Mg content and relatively large size. In the sample containing ferric iron, the M2 is again most compressible with Fe^{3+}-rich M1 and M3 octahedra being stiffer. However, the bulk moduli of all three octahedral sites in Fe-bearing samples are greater than for the Mg-rich end-member (Table 4).

SILICATE SPINEL GROUP

Ringwoodite, the polymorph of Mg_2SiO_4 in the cubic spinel structure (space group *Fd*3*m*; see Figure 3), is presumed to be a major phase in the Earth's Transition Zone at depths of 525 to 670 km (e.g., Ita and Stixrude 1992). This structure features one symmetrically distinct octahedral site at (1/2,1/2,1/2), one tetrahedral site at (1/8,1/8,1/8), and one oxygen at (*u*,*u*,u), where *u* is approximately 0.25. Unlike the olivine form, in which the silicate tetrahedra share edges with the octahedra, the tetrahedron in the spinel structure shares no edges with adjacent octahedra. Although there is evidence for minor amounts of Mg-Si disorder (Hazen et al. 1993), the structures are predominantly normal spinels, in which Mg and Si exclusively occupy the octahedral and tetrahedral sites, respectively. In the high-pressure $(Mg,Fe)_2SiO_4$ system, the spinel form occurs from compositions of pure Fo_{100} to pure Fa_{100}, while high-pressure synthetic silicate spinels are also known with compositions of Ni_2SiO_4, and Co_2SiO_4. In adition, silicate spinels have been reported with up to 2.2 wt % H_2O (Kohlstedt et al 1996, Kudoh and Inoue 1999).

The bulk modulus of ringwoodite (Mg_2SiO_4) has been reported from powder diffraction experiments to 50 GPa as 183 ± 2 GPa (Zerr et al. 1993). Hazen (1993) reported the relative compressibilities of Ni_2SiO_4, Fe_2SiO_4 and ferromagnesian compositions of Fa_{60}, Fa_{78}, and Fa_{80}; however, no atom position data were given in the latter study.

The spinel oxygen *u* parameter reflects the relative size of cation octahedra and tetrahedra. Thus, because the silicate tetrahedron is relatively rigid compared to the divalent cation octahedron, *u* increases with increasing pressure or with decreasing temperature. Finger et al. (1977, 1979) report structure refinements of Ni_2SiO_4 and Fe_2SiO_4 silicate spinels at pressures to 5.5 and 4.0 GPa, respectively, and report site bulk moduli of 170 GPa and >

250 GPa for the octahedron and tetrahedron, respectively. Several refinements of this structure at elevated temperatures have also been reported (Yamanaka 1986, Takeuchi et al 1984). These studies (see Table 4) indicate about three times the volumetric expansion for the octahedron relative to the tetrahedron.

PHENAKITE GROUP

Phenakite (Be_2SiO_4) and willemite (Zn_2SiO_4) are isostructural and have three distinct cation sites, all with tetrahedral coordination. The trigonal structure (space group $R\bar{3}$), illustrated in Figure 4, is a rigid tetrahedral network, rather than a flexible framework. Each oxygen is bonded to *three* tetrahedral cations (one tetravalent and two divalent), rather than two as in a framework. This linkage, and the resulting three-tetrahedra rings, makes the structure much more rigid than a framework. Although the structure of willemite has not yet been studied at elevated temperature or pressure, the structure of phenakite has been investigated at pressures to 4.95 GPa (Hazen and Au 1986) and at several temperatures to 690ºC (Hazen and Finger 1987). At temperature, the structure shows nearly isotropic thermal expansion with the average thermal expansion parallel to *c* being 6.4 x 10^{-6} K^{-1} and expansion perpendicular to *c* being 5.2 x 10^{-6} K^{-1}. These linear expansivities yield an average linear volumetric expansion of 2.44 x 10^{-5} K^{-1}. The volumetric expansivity of the two Be sites are nearly identical at about 2.35 x 10^{-5} K^{-1}, whereas the Si tetrahedron does not show significant expansion over this temperature range.

At pressure, the phenakite structure is relatively incompressible with a bulk modulus of 201 ± 8 GPa and K' of 2 (4). As with expansion, compression is nearly isotropic, with average compressions of the trigonal *a* and *c* axes being 1.63 and 1.53 x 10^{-3} GPa^{-1}, respectively. The behavior of the silicate tetrahedron is similar to that observed in other orthosilicates, with a tetrahedral bulk modulus of 270 ± 40 GPa, while polyhedral moduli of the two symmetrically distinct Be tetrahedra are 230 ± 30 and 170 ± 30 GPa.

CHROMOUS AND CADMIUM ORTHOSILICATES

Although neither occurs as a mineral, chromous and cadmium orthosilicates (Cr_2SiO_4 and Cd_2SiO_4) with the orthorhombic thenardite (Na_2SO_4) structure (space group *Fddd*) (Fig. 5) have been studied at elevated pressures (Miletech et al. 1998, 1999). The divalent cation is in six-fold coordination, which is irregular in the case of Cd but highly distorted in the case of Cr^{2+}. The Cd_2SiO_4 structure was refined as several pressures to 9.5 GPa and has a bulk modulus of 119.5 ± 0.5 GPa with a K' of 6.17(4), whereas the Cr_2SiO_4 structure, refined at several pressures to 9.2 GPa, has a bulk modulus of 94.7 ± 0.5 GPa with a K' of 8.32(14). The lower bulk modulus and larger K' of the chromous structure was attributed by Miletech et al. to compression of the unusually long Cr-O bond and the relatively small size of the Cr^{2+} ion relative to the size of the coordination polyhedron.

GARNET GROUP

Silicate garnets, which occur in many crustal and mantle lithologies, have the general formula $X_3Y_2Si_3O_{12}$, where X is a divalent metal (typically Mg, Fe, Mn, or Ca) and Y is a trivalent metal (typically Al, Fe, or Cr). Garnet, though an orthosilicate, is also framework-like, with a three-dimensional corner-sharing network of tetrahedra and octahedra that define interstitial dodecahedral divalent metal sites with eight coordination. The framework-like behavior of garnet's structural response to temperature and pressure is thus reviewed in this volume by Ross.

The cubic structure (space group *Ia*3*d*), is illustrated in Figure 6. Each oxygen atom in the unit cell is in a symmetrically identical general position that is bonded to one tetrahedrally-coordinated Si, one octahedrally-coordinated trivalent metal, and two eight-coordinated divalent metals. The principal mineral end members are pyrope ($Mg_3Al_2Si_3O_{12}$), almandine ($Fe_3Al_2Si_3O_{12}$), spessartine ($Mn_3Al_2Si_3O_{12}$), grossular ($Ca_3Al_2Si_3O_{12}$), andradite ($Ca_3Fe_2Si_3O_{12}$), and uvarovite ($Ca_3Cr_2Si_3O_{12}$). In addition, a high-pressure polymorph of $MgSiO_3$ called majorite has the garnet structure with formula $Mg_3(MgSi)Si_3O_{12}$. Although pure majorite at low temperature shows a tetragonal distortion to space group $I4_1/a$, these garnets may be cubic at mantle conditions of pressure and temperature. Under temperature and pressure conditions of the Transition Zone, majoritic garnet forms complete crystalline solution with the other aluminous garnets and is thought to be a major constituent of this region of the Earth.

Pyrope garnet has been the subject of more non-ambient structure refinements than any other silicate. Meagher (1975) studied the structures of pyrope and grossular at temperatures to 948 K, while the pyrope structure was documented by Armbruster et al. (1992) from 100 to 293 K, and by Pavese et al. (1995) from 30 to 973 K. Also, volumetric thermal expansivities of several end members have been reported by Skinner (1966) and reviewed by Fei (1995).

The structures of pyrope and grossular were determined at several pressures to 6.0 GPa by Hazen and Finger (1978), and for pyrope and andradite to 19.0 GPa by Hazen and Finger (1989). In addition, Smith (1997) studied the structure of pyrope and a synthetic majorite-bearing garnet at pressures to 13 GPa, while the pyrope structure was documented at pressures up to 33 GPa by Zhang et al. (1998). Equation-of-state parameters of Hazen and Finger (1978) were erroneous, because they combined high-angle, room-pressure unit-cell data on a crystal in air with lower-angle, high-pressure unit-cell data. This procedure resulted in anomalously low bulk moduli. More recent results (Table 7) are fairly consistent, indicating a bulk modulus of 171-179 GPa for pyrope and majoritic garnet and somewhat smaller values for grossular and andradite [see also studies by Leger et al. (1990) and Hazen et al. (1994)]. The study by Zhang et al. (1998) went to very high pressure in a helium pressure medium and was able to constrain K' = 4.4 ± 0.2. They also reported bulk moduli of 107 ± 1 GPa for the Mg site, 211 ± 11 GPa for the Al site and 580 ± 24 GPa for the Si tetrahedron. Smith (1998) reported values of 115, 240 and 430 GPa for these sites in a study of a ferric-iron bearing majoritic garnet to about 13 GPa.

ALUMINOSILICATE GROUP

The Al_2SiO_5 polymorphs, sillimanite, andalusite, and kyanite, are widespread minerals in aluminous rocks of the Earth's crust. The three common polymorphs all have Si in tetrahedral coordination and one Al in octahedral coordination. The second Al is in 4, 5, and 6 coordination in sillimanite, andalusite and kyanite, respectively. The structures are illustrated in Figures 7, 8, and 9, respectively. Sillimanite and andalusite are both orthorhombic, whereas kyanite is triclinic. Liu (1974) reported that kyanite breaks down to Al_2O_3 plus SiO_2 at pressures greater than 16 GPa; however, Ahmad-Zaïd and Madon, (1991) reported a high-pressure phase of composition Al_2SiO_5 and structure similar to V_3O_5, synthesized at pressures in excess of 40 GPa.

The structures of sillimanite and andalusite have been studied at temperatures to 1000ºC and kyanite to 600ºC by Winter and Ghose (1979). Silllimanite has the smallest thermal expansion coefficient (1.46×10^{-5} K^{-1}), whereas those of andalusite and kyanite are about 75% greater. This difference is a consequence of the much lower expansion of the Al in four-coordination in sillimanite, relative to five- and six-coordination polyhedra in andalusite and kyanite, respectively.

The structure of andalusite has been studied at pressures up to 3.7 GPa (Ralph et al. (1984), that of sillimanite to 5.3 GPa (Yang et al. 1997a), and that of kyanite to 4.6 GPa (Yang et al. 1997b). Aluminosilicate compression parameters of the unit cell and structural elements are reviewed in Table 9. In all three structures, the 4+ silicate tetrahedra are the least compressible polyhedra, while 3+ aluminum-bearing polyhedra are more compressible.

ZIRCON

The tetragonal crystal structure (space group $I4_1/amd$) of zircon ($ZrSiO_4$) is illustrated in Figure 10. Zircon, which is isostructural with hafnon ($HfSiO_4$), thorite ($ThSiO_4$) and coffinite ($USiO_4$), features Si in tetrahedral coordination and Zr in distorted eight-fold coordination.

Hazen and Finger (1979) refined the structure of zircon at 8 pressures to 4.8 GPa. They reported a bulk modulus of 227 GPa (with assumed K') of 6.5 or 234 GPa with assumed K' of 4—the highest value reported for a silicate with tetrahedrally-coordinated Si. Note, however, their unit-cell data indicate a K' of approximately –8. Such an anomalous negative K' may have resulted from the merging of high-pressure unit-cell data collected on a crystal in the diamond-anvil cell, with room-pressure data collected on a crystal in air. Such a flawed procedure, which was commonly used before 1980, leads to erroneous equation-of-state parameters (Levien et al. 1979, Hazen and Finger 1989).

The reported bulk modulus of the Si site is 230 ± 40 GPa, which is anomalously compressible relative to SiO_4 tetrahedra in other orthosilicates. By contrast, the bulk modulus of the Zr dodecahedron is 280 ± 40 GPa, which is unusually incompressible for a polyhedron with coordination greater than 6. The 4+ formal charge and relatively large radius of the Zr cation probably accounts for the overall stiffness of the structure and unusually high compression of the Si tetrahedron. The *c* axis of zircon is approximately 70% more compressible than *a*, which reflects the fact that the least compressible Zr-O bonds lie subparallel to the (001) plane. Given the anomalous results of Hazen and Finger (1979), and the improved experimental techniques developed over the past two decades, we recommend that the high-pressure structure of zircon be re-examined.

Unfortunately, no structural data are available for zircon at elevated temperature. However, the unit-cell undergoes anisotropic thermal expansion, with the *c* axis approximately 65% more expansible than *a* (Bayer 1972). Thus, the zircon structure at high temperature appears to display the inverse of its high-pressure behavior.

FUTURE OPPORTUNITIES

This brief overview of high-temperature and high-pressure structural behavior of orthosilicates suggests numerous opportunities for further research. Many of these opportunities arise from the improved instrumentation and data-processing techniques reviewed in this volume.

Other Phases: Several significant orthosilicate mineral structures have not been studied at either elevated temperatures or pressures. We were unable to find structure data at temperature or pressure for magnesium silicate spinels, willemite, the chondrodite group (chondrodite, norbergite, humite, and clinohumite), staurolite, lawsonite, or datolite. None of the hydrous variants of orthosilicates, including hydrous wadsleyites, have been the subject of non-ambient structural studies. Similarly, most of the natural and synthetic isomorphs of olivines (e.g., Ni, Co, Mn, or Ca end members) and garnets (e.g., almandine, spessarite, or uvarovite) have yet to be studied at nonambient conditions. Finally, the previous high-pressure studies on forsterite, fayalite, iron silicate spinel, grossular, andalusite, and zircon are more than 15 years old and do not reflect the present state-of-the-art. In each case cited above, excellent crystals are readily available for study, and investigation to pressures greater than 10 GPa should be relatively straightforward.

Additional High-Temperature Refinements: High-temperature structure refinements are lacking for most orthosilicates, especially for those high-pressure phases thought to occur in the Earth's mantle (e.g., wadsleyites, silicate spinels, majoritic garnets). Indeed, few high-temperature structure refinements of any kind have appeared in the mineralogical literature during the past decade.

Structure Determinations to Pressures o 10 GPa: Most orthosilicates are relatively incompressible; they typically display <1% average linear compression at 5.0 GPa, which is close to the maximum pressure attained by most previous high-pressure structure studies. Details of bond compression (especially Si-O bonds) are, therefore, difficult to resolve over such a limited range. Recent advances in experimental methodologies are permitting studies to pressures greater than 10 GPa and greater precision in pressure measurement. Angel et al. (1997) have shown that measurement of the cell volume of a quartz crystal in the diamond cell with sample can give improved precision of pressure over the use of ruby fluorescence. Such methods are also able to provide significant constraint on the value of K'. The groundbreaking structural study by Zhang et al. (1998) on pyrope to 33 GPa, which employed a helium pressure medium, reveals the greatly enhanced resolution of bond-compression data possible with an expanded pressure range. The high-pressure structures of all orthosilicates could be profitably revisited with the improved techniques described in this volume.

Combined Pressure-Temperature Studies: Structural studies at combined high temperature and pressure, while technically challenging, represent a great opportunity to expand our understanding of orthosilicate crystal chemistry, as well details of equations-of-state, ordering dynamics, and transformation mechanisms. The advent of combined high-temperature and high-pressure techniques for polycrystalline samples (see Fei, this volume) present excellent opportunities for additional studies. Of special interest are the equilibrium ordered states of Mg-Fe orthosilicates under mantle conditions. Recent theoretical calculations (Hazen and Yang, 1999), for example, suggest that cation order-disorder reactions may have a significant effect on pressure-temperature-volume equations-of state of silicate spinels. *In situ* structural determinations present the best opportunity to document these effects.

Application of new and revised experimental apparatus and procedures may lead to insights on several outstanding questions regarding the crystal chemistry of silicates at non-ambient conditions.

The Role of Polyhedral Distortion: To date, only one octahedron or tetrahedron in an orthosilicate – the Li-containing M1 octahedron in $LiScSiO_4$ olivine – displays significant polyhedral distortion as a function of pressure. However, it might be assumed that most cation polyhedra in which some edges are shared would display significant distortions at high pressure. Higher resolution structure refinements over a wider range of pressure or temperature may thus reveal additional examples of significant polyhedral distortion. These data will be essential to understanding the effects of such distortions on equations of state, cation ordering, and phase transition mechanisms.

The Structural Origins of K': For most orthosilicates, refined values of K' are close to 4. There are exceptions, however. The variation of structures with pressure may hold the key to understanding the basis for these variations in K'. It is intuitively reasonable, for example, to expect a relatively high K' in framework structures that experience a stiffening owing to decreasing cation-oxygen-cation angles. Might polyhedral distortions contribute to variations in orthosilicate K'?

The Role of Cation-Cation Repulsion: The bulk modulus-volume relationship for cation polyhedra (see Hazen and Prewitt, this volume) reflects the tendency for larger cations to be more compressible. In several high-pressure orthosilicates, notably Mg-Fe wadsleyites (Hazen et al. 2000a,b) and silicate spinel (Hazen 1993), the iron end-member is significantly less compressible than the Mg end member. High-resolution structure refinements within the pressure stability field of these phases (>10 GPa) might help to resolve this issue.

REFERENCES

Ahmed-Zaïd I, Madon, M (1991) A high pressure form of Al_2SiO_5 as a possible host of aluminum in the lower mantle. Nature 353:683-685

Angel RJ, Allan DR, Miletich R, and Finger LW (1997) The use of quartz as an internal pressure standard in high-pressure crystallography. J Appl Cryst 30:461-466

Armbruster T, Geiger CA, Lager GA (1992) Single-crystal X-ray study of synthetic pyrope and almandine garnets at 100 and 293K. Am Mineral 77:512-521

Artioli G, Rinaldi R, Wilson CC, Zanazzi PF (1995) High-temperature Fe-Mg cation partitioning in olivine: In-situ single-crystal neutron diffraction study. Am Mineral 80:197-200

Bass JD (1995) Elasticity of minerals, glasses, and melts. *In*: TJ Ahrens (ed) Mineral Physics and Crystallography: A Handbook of Physical Constants, p 45-63 American Geophysical Union Reference Shelf 2, Washington, DC

Bayer G (1972) Thermal expansion of ABO_4 compounds with zircon and scheelite structures. J Less-Com Met 26:255-262

Brown GE (1982) Olivines and silicate spinels. *In*: PH Ribbe (ed) Orthosilicates. Rev Mineral 5:275-365

Brown GE, Prewitt CT (1973) High temperature crystal chemistry of hortonolite. Am Mineral 58:577-587

Deer WA, Howie RA, Zussman J (1997) Rock-Forming Minerals Volume 1A: Orthosilicates. 2nd Edition, Geological Society, London

Fei Y (1995) Thermal Expansion. *In*: T.J.Ahrens (ed) Mineral Physics and Crystallography: A Handbook of Physical Constants, p 29-44 American Geophysical Union Reference Shelf 2, Washington, DC

Finger LW, Hazen RM, Yagi T (1977) High-pressure crystal structures of spinel polymorphs of Fe_2SiO_4 and Ni_2SiO_4. Carnegie Inst Wash Yearb 76:504-505

Finger LW, Hazen RM, Yagi T (1979) Crystal structures and electron densities of nickel and iron silicate spinels at elevated temperatures and pressures. Am Mineral 64:1002-1009

Finger LW, Hazen RM, Zhang J, Ko J, Navrotsky A (1993) The effect of Fe on the crystal structure of wadsleyite β-$(Mg_{1-x}Fe_x)_2SiO_4$ ($0 < x \leq 0.40$). Phys Chem Minerals 19:361-368

Hazen RM (1976) Effects of temperature and pressure on the crystal structure of forsterite. Am Mineral 61:1280-1293

Hazen RM (1977) Effects of temperature and pressure on the crystal structure of ferromagnesian olivine. Am Mineral 62:286-295

Hazen RM (1987) High pressure crystal chemistry of chrysoberyl Al_2BeO_4: Insights on the origin of olivine elastic anisotropy. Phys Chem Minerals 14:13-20

Hazen RM (1993) Comparative compressibilities of silicate spinels: anomalous behavior of $(Mg,Fe)_2SiO_4$ Science 259:206-209

Hazen RM, Au AY (1986) High-pressure crystal chemistry of phenakite and bertrandite. Phys Chem Minerals 13:69-78

Hazen RM, Finger LW (1978) Crystal structure and compressibility of pyrope and grossular to 60 kbar. Am Mineral 63:297-303

Hazen RM, Finger LW (1979) Crystal structure and compressibility of zircon at high pressure. Am Mineral 64:196-20

Hazen RM, Finger LW (1980) Crystal structure of forsterite at 40 kbar. Carnegie Inst Wash Yearb 79:364-367

Hazen RM, Finger LW (1982) Comparative Crystal Chemistry. John Wiley & Sons, NewYork

Hazen RM, Finger LW (1987) High-temperature crystal chemistry of phenakite and chrysoberyl. Phys Chem Minerals 14:426-434

Hazen RM, Finger LW (1989) High pressure crystal chemistry of andradite and pyrope: revised procedures for high pressure diffraction experiments. Am Mineral 74:352-359

Hazen RM, Yang H. (1999) Effects of cation substitution and order disorder on P-V-T equations of state of cubic spinels. Am Mineral 84:1956-1960

Hazen RM, Zhang J, Ko J (1990) Effects of Fe/Mg on the compressibility of synthetic wadsleyite: β-$(Mg_{1-x}Fe_x)_2SiO_4$ ($x \leq 0.25$). Phys Chem Minerals 17:416-419

Hazen RM, Downs RT, Finger LW, Ko J (1993) Crystal chemistry of ferromagnesian silicate spinels: evidence for Mg-Si disorder. Am Mineral 78:1320-1323

Hazen RM, Downs RT, Conrad PG, Finger LW, Gasparik T (1994) Comparative compressibilities of majorite-type garnets. Phys Chem Minerals 21:344-349

Hazen RM, Downs RT, Finger LW (1996) High-pressure crystal chemistry of $LiScSiO_4$, an olivine with nearly isotropic compression. Am Mineral 81:327-334

Hazen RM, Weingerger MB, Yang H, Prewitt CT (2000a) Comparative high pressure crystal chemistry of wadsleyite, β-$(Mg_{1-x}Fe_x)_2SiO_4$ (x=0 and 0.25) Am Mineral 85 (in press)

Hazen RM, Yang H, Prewitt CT (2000b) High-pressure crystal chemistry of Fe^{3+}-wadsleyite, β-$Fe_{2.33}Si_{0.67}O_4$ Am Mineral 85 (in press)

Hirschmann M (1992) "Studies of nickel and minor elements in olivine and in silicate liquids" Ph.D Thesis, University of Washington, Seattle, 166 pp

Horioka K, Takahashi K, Morimoto N, Horiuchi H, Akaogi M, Akimoto S (1981a) Structure of nickel aluminosilicate (Phase IV): A high pressure phase related to spinel. Acta Cryst B37:635-638

Horioka K, Nishiguchi M, Morimoto N, Horiuchi H, Akaogi M, Akimoto S (1981b) Structure of nickel aluminosilicate (Phase V): A high pressure phase related to spinel. Acta Cryst B37:638-640

Inoue T, Yurimoto Y, Kudoh Y (1997) Hydrous modified spinel $Mg_{1.75}SiH_{0.5}O_4$: a new water reservoir in the Transition Region. Geophys Res Lett 22:117-120

Ita J, Stixrude L (1992) Petrology, elasticity, and composition of the mantle transition zone. J Geophys Res 97:6849-6866

Kolstedt DL, Keppler H, Rubie DC (1996) The solubility of water in α, β, and γ phases of $(Mg,Fe)_2SiO_4$. Contrib Mineral Petrol 123:345-357

Kudoh Y, Takeda H (1986) Single crystal X-ray diffraction study on the bond compressibility of fayalite, Fe_2SiO_4 and rutile, TiO_2 under high pressure. Physica 139 & 140B (1986) 333-336

Kudoh Y, Takéuchi T (1985) The crystal structure of forsterite Mg_2SiO_4 under high pressure up to 149 kbar. Z Krist 117:292-302

Kudoh Y, Inoue T (1999) Mg-vacant structural modules and dilution of symmetry of hydrous wadsleyite β-$Mg_{2-x}SiH_xO_4$ with $0.00 < x < 0.25$. Phys Chem Minerals 26:382-388

Lager GA, Meagher EP (1978) High temperature structure study of six olivines. Am Mineral 63:365-377

Leger JM, Redon AM, Chateau C (1990) Compressions of synthetic pyrope, spessartine and uvarovite garnets up to 25 GPa. Phys Chem Minerals 17:157-161

Levien L, Prewitt CT, Weidner DJ (1979) Compression of pyrope. Am Mineral 64:895-808

Liu LG, (1974) Disproportionation of kyanite into corundum plus stishovite at high temperature and pressure. Earth Plan Sci Lett 24:224-228

Ma C-B, Sahl K, Tillmanns E (1975) Nickel aluminosilicate, phase I. Acta Cryst B31:2137-2139

Ma C-B, Tillmanns E (1975) Nickel aluminosilicate, phase II. Acta Cryst B31:2139-2141

Ma C-B, Sahl K (1975) Nickel aluminosilicate, phase III. Acta Cryst B31:2142-2143

Meagher EP (1975) the crystal structures of pyrope and grossular at elevated temperatures. Am Mineral 60:218-228

Miletich R, Seifert F, Angel RJ (1998) Compression of cadmium orthosilicate, Cd_2SiO_4: a high pressure single-crystal diffraction study. Z Krist 213:288-295

Miletich R, Nowak M, Seifert F, Angel RJ, Brandstätter G (1999) High-pressure crystal chemistry of chromous orthosilicate, Cr_2SiO_4. A single-crystal X-ray diffraction and electronic absorption spectroscopy study. Phys Chem Minerals 26:446-459

Motoyama T, Matsumoto T (1989) The crystal structure and the cation distributions of Mg and Fe in natural olivines. Min J 14:338-350

Pavese A, Artioli G, Prescipe M (1995) X-ray single-crystal diffraction study of pyrope in the temperature range 30-973K. Am Mineral 80:457-464

Ralph RL, Finger LW, Hazen RM, Ghose S. (1984) Compressibility and crystal structure of andalusite at high pressure. Am Mineral 69:513-519

Redfern SAT, Henderson CMB, Knight KS, Wood BJ (1997) High temperature order-disorder in $(Fe_{0.5}Mn_{0.5})_2SiO_4$ and $(Mg_{0.5}Mn_{0.5})_2SiO_4$ olivines: an in situ neutron diffraction study. Eur J Mineral 9:287-300

Sharp ZD, Hazen RM, Finger LW (1987) High pressure crystal chemistry of monticellite $CaMgSiO_4$. Am Mineral 72:748-755

Skinner BJ (1966) Thermal expansion. *In*: SP Clark (ed) Handbook of physical constants, p 75-95, Geol Soc Am Mem, New York

Smith HM (1997) "Ambient and high pressure single-crystal X-ray studies of pyrope and synthetic ferric majorite" Ph.D. Thesis, University of Colorado, Boulder, 119pp

Smyth JR (1975) High temperature crystal chemistry of fayalite. Am Mineral 60:1092-1097

Smyth (1987) β-Mg_2SiO_4: a potential host for water in the mantle? Am Mineral 72:1051-1055

Smyth JR, Hazen RM (1973) The crystal structures of forsterite and hortonolite at several temperatures up to 900ºC. Am Mineral 58:588-593

Smyth JR, Kawamoto T (1997) Wadsleyite II: a new high pressure hydrous phase in the peridotite-H_2O system. Earth Planet Sci Lett 146:E9-E16

Smyth JR, Tafto J (1982) Major and minor element ordering in heated natural forsterite. Geophys Res Lett 9:1113-1116

Smyth JR, Kawamoto T, Jacobsen SD, Swope RJ, Hervig RL, Holloway J (1997) Crystal structure of monoclinic hydrous wadsleyite [β-$(Mg,Fe)_2SiO_4$]. Am Mineral. 82:270-275

Sasaki S, Prewitt CT, Sato Y, and Ito E (1982) Single crystal X-ray study of γ-Mg_2SiO_4. J Geophys Res 87:7829-7832

Suzuki (1975) thermal expansion of periclase and olivine and their anharmonic properties. J Phys Earth 23:145-159

Suzuki I, Ohtani E, Kumazawa M (1980) Thermal expansion of modified spinel, β-Mg_2SiO_4. J Phys Earth 28:273-280

Suzuki I, Ohtani E, Kumazawa M (1979) Thermal expansion of spinel, γ-Mg_2SiO_4. J Phys Earth 27:63-69

Takéuchi T, Yamanaka T, Haga H, Hirano (1984) High-temperature crystallography of olivines and spinels. *In*: I Sunagawa (ed) Materials Science of the Earth's Interior, p 191-231, Terra, Tokyo

Winter JK, Ghose S (1979) Thermal expansion and high temperature crystal chemistry of the Al_2SiO_5 polymorphs. Am Mineral 64:573-586

Yamanaka T (1986) Crystal structures of Ni_2SiO_4 and Fe_2SiO_4 as a function of temperature and heating duration. Phys Chem Minerals 13:227-232

Yang H, Hazen RM, Finger LW, Prewitt CT, Downs RT (1997a) Compressibility and crystal structure of sillimanite at high pressure. Phys Chem Minerals 25:39-47

Yang H, Downs RT, Finger LW, Hazen RM (1997b) Compressibility and crystal structure of kyanite Al_2SiO_5 at high pressure. Am Mineral 82:467-474

Zhang L, Ahsbahs H, Kutoglu A (1998) Hydrostatic compression and crystal structure of pyrope to 33 GPa. Phys Chem Minerals 25:301-307

Zerr A, Reichmann H-J, Euler H, Boehler R (1993) Hydrostatic compression of γ-$(Mg_{0.6}Fe_{0.4})_2SiO_4$ to 50.0 GPa. Phys Chem Minerals 19:507-509.

Table 1. Linear thermal expansion coefficients for olivine structure components.

End-Member	Forsterite	Fayalite	Liebenbergite	Monticellite	Glaucochroite	Chrysoberyl
Formula	Mg_2SiO_4	Fe_2SiO_4	Ni_2SiO_4	$CaMg_{0.93}Fe_{0.07}SiO_4$	$Ca_{0.98}Mn_{0.87}Mg_{0.10}SiO_4$	Al_2BeO_4
Sample	Synthetic	Synthetic	Synthetic	Natural	Natural	Natural
T range	23-1600ºC	20-900ºC	25-900ºC	25-795ºC	25-800ºC	25-690ºC
Unit cell						
αV (x 10^{-5} K^{-1})	4.36	3.19	3.44	2.97	3.17	2.39
αa (x 10^{-5} K^{-1})	1.12	0.99	1.19	1.01	1.05	0.74
αb (x 10^{-5} K^{-1})	1.67	0.95	1.11	0.99	1.00	0.85
αc (x 10^{-5} K^{-1})	1.46	1.19	1.12	1.13	1.09	0.83
Polyhedral Volumes	(x 10^{-5} K^{-1})					
M1	4.32	2.88	4.19	4.68	4.55	2.25
M2	5.07	4.51	3.68	3.62	4.01	3.89
T	0	-1.17	0.36	-1.23	-2.13	2.57
NPV	4.40	3.37	3.33	3.20	2.81	1.99
Reference	Takeuchi et al. (1984)	Smyth (1975)	Lager & Meagher (1978)	Lager & Meagher (1978)	Lager & Meagher (1978)	Hazen and Finger (1987)

Table 2. Linear thermal expansion coefficients for intermediate-compositions olivine structure components.

Composition	$Fo_{88}Fa_{12}$	$Fo_{70}Fa_{30}$	$Fo_{13}Fa_{87}$	$Fo_{50}Te_{50}$	$Fa_{50}Te_{50}$
Formula	$Mg_{1.76}Fe_{0.24}SiO_4$	$Mg_{1.40}Fe_{0.60}SiO_4$	$Mg_{0.26}Fe_{1.74}SiO_4$	$Mg_{1.00}Mn_{1.00}SiO_4$	$Fe_{1.00}Mn_{1.00}SiO_4$
Sample	Natural	Natural	Natural	Synthetic	Synthetic
T range	23-1060ºC	20-700ºC	20-600ºC	20-1000ºC	20-1000ºC
Unit cell					
αV (x 10^{-5} K^{-1})	3.85	3.60	3.38	3.52	3.38
αa (x 10^{-5} K^{-1})	0.61	0.95	0.93	1.10	0.95
αb (x 10^{-5} K^{-1})	1.41	1.28	1.03	1.18	1.08
αc (x 10^{-5} K^{-1})	1.78	1.34	1.39	1.19	1.31
Polyhedral Volumes	(x 10^{-5} K^{-1})				
M1	3.45	3.96	3.96	5.17	4.03
M2	4.82	4.15	3.60	2.82	2.95
Si	n.r.	-0.20	-0.23	0.64	0.82
Npv	n.r.	3.53	3.33	3.43	3.45
Reference	Artioli et al. (1995)	Motoyama & Matsumoto (1989)	Motoyama & Matsumoto (1989)	Redfern et al. (1997)	Redfern et al. (1997)

Table 3. Compression of olivine structures at 300K.

End-member	Forsterite	Forsterite	Fayalite	Fayalite	Monticellite	Chrysoberyl	
Formula	Mg_2SiO_4	Mg_2SiO_4	Fe_2SiO_4	$Fe_{1..94}Mn_{0.11}Mg_{0.04}SiO_4$	$Ca_{0.99}Mg_{0.91}Fe_{0.09}SiO_4$	Al_2BeO_4	$LiScSiO_4$
Sample	Synthetic	Synthetic	Synthetic	Natural	Natural	Natural	Synthetic
Pmax (GPa)	5.0	14.9	4.2	14.0	6.2	6.25	5.6
K_{T0} (GPa)	132	123	113	132	113	242	118
K'	4.0 (fixed)	4.3	4 (fixed)	4 (fixed)	4 (fixed)	4 (fixed)	4 (fixed)
Axial Compressions	(10^{-3} GPa^{-1})						
β*a*	1.6	1.5	0.8	1.2	1.96	1.09	2.70
β*b*	4.3	2.8	5.8	4.0	3.62	1.47	2.80
β*c*	0.8	2.7	1.4	1.3	2.05	1.32	2.61
Site bulk moduli (GPa)							
M1	120	140		130	150	180	84
M2	100	130		130	110	300	204
Si	>550	190	>500	>400	>300	300	315
Reference	Hazen (1976)	Kudoh & Takeuchi (1985)	Hazen (1977)	Kudoh & Takeda (1986)	Sharp et al. (1987)	Hazen (1987)	Hazen et al. (1996)

Table 4. Thermal Expansion parameters of silicate spinels and spinelloids.

End-Member	Wadsleyite	Fe_2SiO_4 – spinel	Ni_2SiO_4 – spinel
Formula	$Mg_3Al_2Si_3O_{12}$	Fe_2SiO_4	Ni_2SiO_4
Sample	Synthetic	Synthetic	Synthetic
T range	20-800ºC	20-700ºC	20-700ºC
Unit cell			
αV (x 10^{-5} K^{-1})	3.10	5.55	2.55
αa (x 10^{-5} K^{-1})	1.48	1.83	0.84
αb (x 10^{-5} K^{-1})	0.66		
αc (x 10^{-5} K^{-1})	0.90		
Polyhedral Volumes	(x 10^{-5} K^{-1})		
X	N/r	6.3	3.3
Si	N/r	3.9	0.94
NPV			
Reference	Suzuki et al. (1980)	Yamanaka (1986)	Yamanaka (1986)

Table 5. Compression of silicate spinels and spinelloid structures.

Structure	Wadsleyite	Wadsleyite	Spinelloid III	Spinel	Spinel
Formula	Mg_2SiO_4	$Mg_{1.50}Fe_{0.50}SiO_4$	$Fe^{2+}_{1.67}Fe^{3+}_{0.33}(Fe^{3+}_{0.33}Si_{0.67})O_4$	Ni_2SiO_4	Fe_2SiO_4
Sample	Synthetic	Synthetic	Synthetic	Synthetic	Synthetic
Pmax (GPa)	10.12	10.12	8.95	5.5	4.0
K_{T0} (GPa)	172 (3)	173 (3)	173 (3)	227(4)	196(8)
K'	6.3 (7)	7.1 (8)	5.2 (9)	4 (fixed)	4 (fixed)
Axial Compressions	(10^{-3} GPa^{-1})				
β*a*	1.45(2)	1.43	1.79	1.23	1.67
β*b*	1.46 (3)	1.41	1.53		
β*c*	2.00(4)	1.97	1.80		
Site bulk moduli (GPa)					
M1	146 (8)	188 (15)	202 (10)	170(10)	244(20)
M2	137 (13)	126 (10)	163 (12)		
M3	149 (7)	166 (6)	185 (17)		
Si	350 (60)	340(38)	315 (47)	>250	>120
Reference	Hazen et al. (2000a)	Hazen et al. (2000a)	Hazen et al. (2000b)	Finger et al. (1979)	Finger et al. (1979)

Table 6. Linear thermal expansion parameters of garnet structures

End-Member	Pyrope	Grossular
Formula	$Mg_3Al_2Si_3O_{12}$	$Ca_3Al_2Si_3O_{12}$
Sample	Synthetic	Natural
T range	25-700ºC	25-675ºC
Unit cell		
αV (x 10^{-5} K^{-1})	3.15	2.69
αa (x 10^{-5} K^{-1})	1.04	0.89
Polyhedral Volumes	(x 10^{-5} K^{-1})	
X	4.21	2.37
Y (Al)	3.03	3.79
Si	1.36	2.10
NPV	2.67	2.75
Reference	Pavese et al (1995)	Meagher (1975)

Table 7. Compression of garnet structures at 300K.

End-member	Pyrope	Pyrope	Pyrope	Grossular	Andradite	Majorite
Formula	$Mg_3Al_2Si_3O_{12}$	$Mg_3Al_2Si_3O_{12}$	$Mg_{2.84}Fe_{0.10}Ca_{0.06}Al_2Si_3O_{12}$	$Ca_3Al_2Si_3O_{12}$	$Ca_3Fe_2Si_3O_{12}$	$(Mg_{2.79}Fe_{0.03}Ca_{0.19})(Mg_{0.38}Fe_{0.30}Al_{0.78}Si_{0.52})Si_3O_{12}$
Sample	Natural	Synthetic	Natural	Natural	Natural	Synthetic
Pmax (GPa)	5.6	33.4	9.9	6.1	19.0	12.9
K_{T0} (GPa)	179	171(2)	176	135(5)	159(2)	172
K'	4 (fixed)	4.4(2)	4 (fixed)	4 (fixed)	4 (fixed)	4 (fixed)
Axial Compressions	(10^{-3} GPa^{-1})					
βa	1.56	1.39	1.67			1.58
Site bulk moduli (GPa)						
X	130(10)	107(1)	119(10)	115(13)	160	116(4)
Y (Al)	220(50)	211(11)	137(40)	220(50)	330(33)	189(21)
Z (Si)	300(100)	580(24)	>500	300(100)	200(20)	403(118)
Reference	Hazen & Finger (1989)	Zhang et al. (1998)	Smith (1997)	Hazen & Finger (1978)	Hazen & Finger (1989)	Smith (1997)

Table 8. Linear thermal expansion parameters of the aluminosilicate structures.

End-Member	Sillimanite	Andalusite	Kyanite
Molar Volume (cm^3)	50.035	51.564	44.227
Sample	Natural	Natural	Natural
T range	25-1000ºC	25-1000ºC	25-800ºC
Unit cell			
αV (x 10^{-5} K^{-1})	1.46	2.48	2.60
αa (x 10^{-5} K^{-1})	0.208	1.310	0.770
αb (x 10^{-5} K^{-1})	0.773	0.913	0.652
αc (x 10^{-5} K^{-1})	0.472	0.238	1.061
Polyhedral Volumes	(x 10^{-5} K^{-1})		
Al1 (x 10^{-5} K^{-1})	1.86	3.36	3.29
Al2 (x 10^{-5} K^{-1})	0.85	1.97	2.70
Al3 (x 10^{-5} K^{-1})			2.75
Al4 (x 10^{-5} K^{-1})			1.76
Si 1 (x 10^{-5} K^{-1})	0.74	0.09	0.47
Si 2 (x 10^{-5} K^{-1})			0.78
NPV (x 10^{-5} K^{-1})	1.45	2.43	2.67
Reference	Winter and Ghose (1979)	Winter and Ghose (1979)	Winter and Ghose (1979)

Table 9. Compression of Aluminosilicate structures

End-member	Sillimanite	Andalusite	Kyanite
Formula	Al_2SiO_5	Al_2SiO_5	Al_2SiO_5
Sample	Synthetic	Synthetic	Synthetic
Pmax (GPa)	5.29	3.7	4.56
K_{T0} (GPa)	171(1)	151	193
K'	4(3)	4 (fixed)	4 (fixed)
Axial Compressions	(10^{-3} GPa^{-1})		
βa	1.80	3.23	1.70
βb	2.49	2.24	1.55
βc	0.99	1.48	1.73
Site bulk moduli (GPa)			
Al1	162	130	274
Al2	269	160	207
Al3			224
Al4			281
Si1	367	410	322
Si2			400
Reference	Yang et al. (1997a)	Ralph et al. (1984)	Yang et al. (1997b)

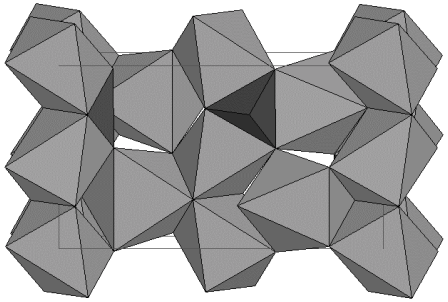

Figure 1. Polyhedral representation of the crystal structure of olivine (*a*-axis projection, *b*-horizontal).

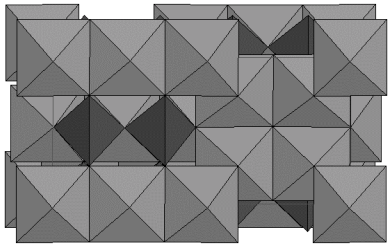

Figure 2. Polyhedral representation of the crystal structure of wadsleyite (*c*-axis projection, *b*-horizontal).

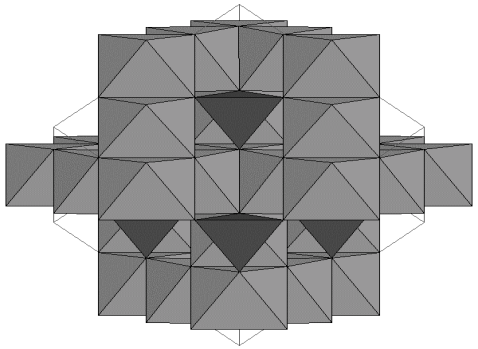

Figure 3. Polyhedral representation of the crystal structure of ringwoodite ([111]- projection).

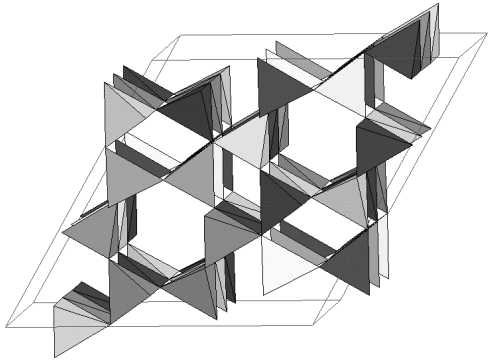

Figure 4. Polyhedral representation of the crystal structure of phenakite (Be_2SiO_4) (*c*-axis projection, *b*-horizontal). All cations are in tetrahedral coordination with each oxygen bonded to three tetrahedral cations.

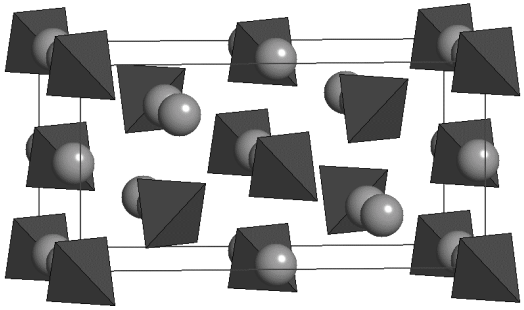

Figure 5. Polyhedral representation of the crystal structure of Cd-orthosilicate (thenardite structure) (*a*-axis projection, *b*-horizontal). The divalent cation is in highly irregular six-fold coordination.

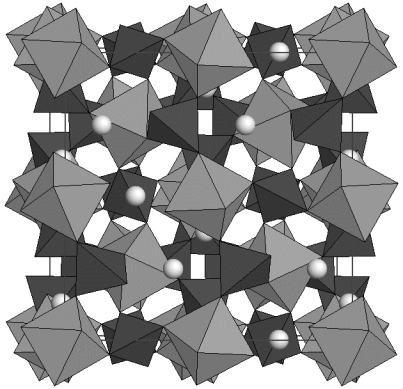

Figure 6. Polyhedral representation of the crystal structure of garnet. The structure is a framework of corner-sharing tetrahedra (Si) and octahedra (Al, Fe^{3+} or Cr), with interstitial divalent metals (Mg, Fe^{2+}, Ca or Mn) shown as spheres.

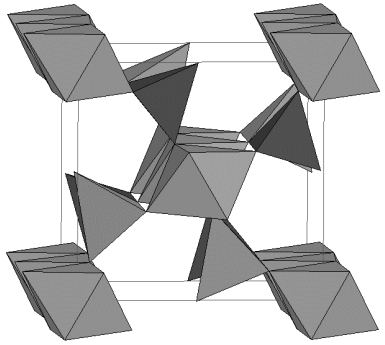

Figure 7. Polyhedral representation of the crystal structure of sillimanite (*c*-axis projection, *b*-horizontal). The structure is composed of bands of edge-sharing Al octahedra parallel to *c* connected by alternating Al and Si tetrahedra.

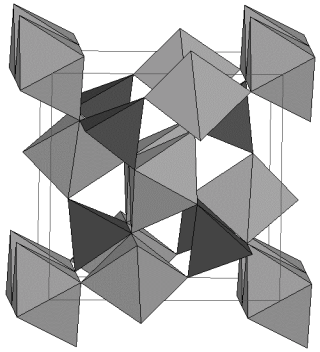

Figure 8. Polyhedral representation of the crystal structure of andalusite (*c*-axis projection, *b*-horizontal). The structure is composed of bands of edge-sharing Al octahedra parallel to *c* connected by Al trigonal bi-pyramids and Si tetrahedra.

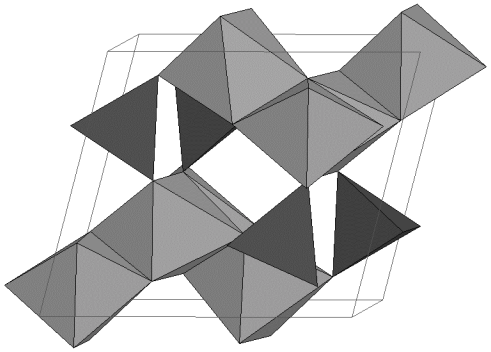

Figure 9. Polyhedral representation of the crystal structure of kyanite (*c*-axis projection, *b*-horizontal). The structure is composed of bands of edge-sharing Al octahedra parallel to *c*, connected by Al octahedra and Si tetrahedra.

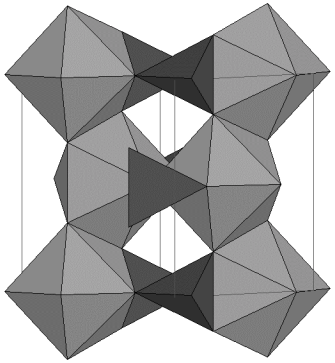

Figure 10. Polyhedral representation of the crystal structure of zircon ([110] -projection, *c*-vertical). The structure is composed of eight-coordinated Zr and Si tetrahedra.